24th International Conference on Renewable Energies and Power Quality (ICREPQ'26)
Santander (Spain), 10th to 12th June 2026
ISBN-13: 978-84-09-82044-3

Modelling the Temperature-Dependent AC Resistance of Two-Layer Steel-Core Conductors for DLR Applications

A. Soni[1,2], J.-R. Riba[2] and M. Moreno-Eguilaz[2]

[1] SICAME-Spain, Sant Esteve Sesrovires, Spain
[2] Electrical Engineering Department, Universitat Politècnica de Catalunya, Terrassa, Spain. jordi.riba-ruiz@upc.edu

Abstract. Steel-cored conductors, and specifically aluminum conductors steel-reinforced (ACSR), are widely applied in overhead power lines. However, because of the magnetization of the steel core, such conductors exhibit a non-linear electrical behavior, and their electrical resistance depends on the intensity of the current flowing through the conductor. This paper analyzes the alternating current (AC) resistance of two-layer ACSR conductors. It compares different formulations to predict their AC resistance and concludes that the existing formulations fail in predicting the current dependency of the AC resistance in the lower current range. The results presented here show that the magnetic flux generated by the two aluminum layers is not completely cancelled out, although the two layers are stranded in opposite directions. It is also shown that this effect is more pronounced at low current levels.

Key words. Conductors, steel core, power lines, power loss, dynamic line rating, ampacity.

1. Introduction

Aluminum conductors steel-reinforced (ACSR) are widely used in distribution and transmission overhead power lines. Dynamic line rating (DLR) is a new technology aligned with smart and digital grid applications that determines in real-time the current-carrying capacity or ampacity of transmission lines based on actual environmental conditions. Contrarily to the traditional static line rating (SLR) approach, which typically assumes a worst-case scenario to set a safe ampacity limit, DLR replaces these conservative estimates with live data. Therefore, DLR maximizes power line capacity by adjusting for real-time weather conditions without compromising thermal limits [1]. DLR needs accurate conductor models to predict the temperature of the conductor and thus the sag, since the minimum distance of the conductor to ground is a safety red line, because it never should be below the legal clearance limit. It is known that resistive losses are the main source of heating in bare conductors used in overhead power lines, so DLR requires the alternating current (AC) resistance of the conductors to be accurately modeled.

ACSR conductors have a core formed of galvanized steel wires surrounded by one or more layers of aluminum strands. These aluminum layers are helically wound in opposite directions around the core [2]. This contra-helical laying is essential for the mechanical and electrical stability of an ACSR conductors. From a mechanical perspective, by reversing the direction of each layer, the torsional torques cancel each other out, thus keeping the conductor balanced, preventing it from bird-caging. The steel core in ACSR conductors provides the mechanical strength to the conductors, and the highly conductive aluminum strands provide low resistance path for current conduction.

The AC resistance of ACSR conductors is usually higher than the corresponding direct current (DC) resistance due to several factors, such as the induced eddy currents that do not occur under DC supply, and due to the effect of the magnetic steel core. The nonlinear behavior of the magnetic steel core is the responsible that the AC resistance of ACSR conductors is not only temperature dependent, but also current dependent [3]. This nonlinear behavior makes it very challenging to develop accurate models to predict the AC resistance of such conductors. It is known that the current flows following the spiral path of the aluminum strands [4], [5]. Similarly to a solenoid, this spiral current generates an axial component of the internal magnetic field. According to the bibliography, this effect depends on the number of layers of the conductor, being at its maximum for single-layer conductors, and almost cancelling out in the case of two-layer conductors because of the contra-helical laying directions of adjacent layers [6], [7]. The effective axial component of the magnetic flux inside the conductor changes the current distribution in the aluminum layers, thus producing eddy current and hysteresis losses [1], [8], [9], which in turn increase the AC resistance and temperature [2]. The magnitude of this effect, known as transformer effect, is highly dependent on the axial flux intensity, which in turn depends on the magnetic properties of the steel core and on the amplitude of the current flowing through the conductor [10]. Another difficulty is that the magnetic flux density within the core contains harmonics, thus making the problem even more challenging.

In this paper, we study two-layer ACSR conductors and we examine two methods found in the literature to model the AC resistance of such conductors. These methods are compared against the 4-wire Kelvin method that is considered the reference method. The experimental results presented here reveal that even in two-layer conductors, the AC resistance depends on the current level, this effect being notorious at low current levels and decreasing as high current levels. It is also shown that the methods for modelling the AC resistance of steel-core conductors found in the literature do not provide an accurate representation of this phenomenon, at least for low current levels, while the 4-wire Kelvin method is more accurate but difficult to apply in operating power lines.

2. Modelling of the AC Resistance

The complex relative permeability of the steel core is represented as follows [2],

$$\overline{\mu}_r = \mu_r' - j\mu_r'' = \frac{B_p}{\mu_0 H_p} e^{-j\delta} \quad (1)$$

$\mu_0 = 4\pi 10^{-7}$ H/m being the permeability of free space, B_p [T] the magnetic flux density (peak value) and H_p [A/m] the magnetic field (peak value). Note that $\overline{\mu}_r = \mu_r' - j\mu_r''$ is a dimensionless complex quantity. Its real part, μ_r' [-], represents the reactive component due to the magnetic energy stored in the material. Its imaginary part, μ_r''[-], is related to the magnetic losses in each hysteresis cycle, representing the electrical energy that is converted to heat.

The loss angle of the steel core material, δ[º], is an important parameter, representing the phase difference between fields H and B, which can be determined as follows [4], [11],

$$\delta = \tan^{-1}(\mu_r''/\mu_r') \quad (2)$$

ACSR conductors are made of aluminum wires which helically wound around the steel wires of the conductor core. Therefore, this arrangement is similar to a magnetic coil with a lossy core. This arrangement presents a direct current (DC) resistance R_{DC} [Ω/m] due to the aluminum strands and an inductance L [H/m] due to the effective coil which can be determined as [12],

$$L = \mu_r' \mu_0 A_s n^2 \text{ [H/m]} \quad (3)$$

A_s [m^2] being the steel core cross-sectional, n [m^{-1}] the effective number of turns per meter of the aluminum wires around the steel core (spiral geometry), which due to the two layers, can be approximated by the following expression [13],

$$n = \frac{\sum_{i=1}^{num\_layers} \frac{n_{\text{Al,i}}}{\lambda_i}(-1)^i}{n_{\text{Al,,total}}} \text{ [turns/m] [H/m]} \quad (4)$$

where *num_layers* refers to the number of aluminum layers, λ_i is the lay length of layer i, $n_{\text{Al,total}}$ is the number of Al strands in the conductor and $n_{\text{Al,i}}$ is the number of Al strands in layer i, with $i = 1,2$.

According to [12], [13], the resistance of the steel core can be calculated as follows,

$$R_{core} = \omega L \tan\delta \text{ [Ω/m]} \quad (5)$$

$\omega = 2\pi f$ [rad/s] being the angular frequency, $f = 50$ Hz the power frequency, and L [H/m] is the inductance as in (3).

Finally, helically stranded steel-cored conductors exhibit an alternating current (AC) impedance given by [13],

$$\overline{Z}_{AC} = (R_{DC,Al} + R_{eddy,Al} + \underbrace{\omega L \tan\delta}_{R_{core}}) + j\omega L \text{ [Ω/m]} \quad (6)$$

$R_{DC,Al}$ being the DC resistance of the conductor, and $R_{eddy,Al}$ the resistance term due to the eddy currents occurring in the aluminum wires. The real part in (6) accounts for the resistance term, which can be written as,

$$R_{AC} = R_{DC,Al} + R_{eddy,Al} + \omega L \tan\delta \text{ [Ω/m]} \quad (7)$$

Equation (7) uses a series summation of loss-related resistance terms to arrive at the final R_{AC} value. According to Cigré [13], the eddy current term is negligible in front of the other two terms, so that (7) can be rewritten as,

$$R_{AC} \approx R_{DC,Al} + \omega L \tan\delta = R_{DC,Al} + 2\pi f \left|\overline{\mu}_r'\right| \mu_0 A_s n^2 \tan\delta \text{ [Ω/m]} \quad (8)$$

Therefore, (8) can be used to determine R_{AC}, which must be always greater than R_{DC}.

3. Two Proposed Methods to Determine the AC resistance

According to (8), in order to estimate R_{AC}, the values of parameters μ_r' and δ must be known. However, as deduced from (1), μ_r' and δ are related by mean of the B and H fields. Due to the non-linear behavior of the steel core, the field B and H contain harmonics, and specially the field B. Therefore, it is difficult to determine μ_r' and δ. Next subsections propose two methods to determine R_{AC}.

A. Method #1

Method #1 calculates $\mu_{r,eff}$ and δ_{eff} from the energy losses in the steel core due to the hysteresis cycle but excludes the transformer effect. The real value of $\mu_{r,eff}$ is determined as follows,

$$\mu_{r,eff} = \frac{B_{RMS}}{\mu_0 H_{RMS}} \quad (9)$$

where RMS refers to the root-mean square value. Then, the energy loss in one hysteresis cycle is determined as,

$$E_{loss} = \int HdB \text{ [J/m}^3\text{]} \quad (10)$$

Next, the effective loss angle, δ_{eff}, is determined as,

$$\delta_{eff} = \tan^{-1}\left(\frac{E_{loss}}{2\pi E_{mag}}\right) \quad (11)$$

where E_{mag} is the maximum value of the energy stored per cycle in the material, which can be calculated as,

$$E_{mag} = \max\left[\frac{1}{2} B(t) H(t)\right] \text{ [J/m}^3\text{]} \quad (12)$$

Finally, the value of R_{AC} can be determined from (8).

B. Method #2

Barrett *et al.* [8], based on previous work published in [13] developed a method to determine the AC resistance in steel-cored conductors that considers the power losses within the core and the current redistribution due to the transformer effect. This method was adapted in [13].

This method takes into account the complex value of the relative magnetic permeability, so it considers the core losses. Method #2 proposes a conductor model based on DC resistances, and inductances. The inductances are due to both the longitudinal and circular magnetic flux components [8].

Fig. 1 depicts the two-layer conductor with the equalizers used to measure the voltage drop across the length of 1 m, as well as the equivalent circuit model of the conductor.

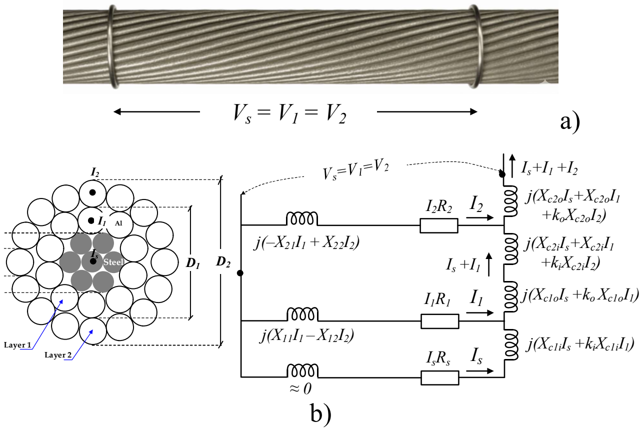

Fig. 1. a) Two-layer steel-core conductor. b) Conductor layout and impedance model of the conductor considering the steel core and two aluminum layers.

Note that in Fig.1, X_{ij} [Ω/m] are the mutual reactances between layer *i* and *j* due to the longitudinal flux component, X_{ci} and X_{co} [Ω] refer to the reactances due to the circular flux component and R_s, R_1 and R_2 [Ω/m]are the DC resistances of the different conductor layers. These parameters can be determined as follows,

$$\begin{cases} X_{c1i} = \mu_0 f \ln[(D_1 - d)/D_s] \\ X_{c1o} = \mu_0 f \ln[D_1/(D_1 - d)] \\ X_{c2i} = \mu_0 f \ln[(D_2 - d)/D_1] \\ X_{c2o} = \mu_0 f \ln[D_2/(D_2 - d)] \\ R_1 = \dfrac{\rho_{Al}}{n_1(\pi/4)d^2}\left(1 + [\pi(D_1 - d)/\lambda_1]^2\right)^{1/2} \\ R_2 = \dfrac{\rho_{Al}}{n_2(\pi/4)d^2}\left(1 + [\pi(D_2 - d)/\lambda_2]^2\right)^{1/2} \\ R_s = \dfrac{\rho_{steel}}{n_s(\pi/4)d_s^2}\left(1 + [\pi D_s/\lambda_s]^2\right)^{1/2} \\ X_{ij} = X_{ji} = 2\pi f[\mu_0 \overline{\mu}_{rs} A_s + \mu_0(A_{L,ij} - A_s)]/(\lambda_i \lambda_j) \; i = 1,2 \\ \text{where } A_{L,ij} = (\pi/4)(D_i - D_j)^2, \; A_s = (\pi/4)D_s^2 \\ k_i = 0.29, \; k_o = 0.71 \end{cases} \quad (13)$$

Since $\overline{\mu}_{rs}$ is a complex number, X_{ij} [Ω] also results in a complex value.

Note that I_{total} is known since it is a measured value, while $V_s = V_1 = V_2$ can be determined from the system of equations arising from solving the circuit in Fig. 1b. Therefore, R_{AC} can be calculated as,

$$R_{AC} = \text{real}(V_s / I_{total}) \quad (14)$$

C. Reference 4-wire method

In order to assess the accuracy of the results provided by Methods #1 and #2, a reference method is needed. To this end, the four-wire method was taken as the reference method, as it is widely applied and referenced in Cigré [14]. It is based on injecting a known current I_{AC} and measuring the voltage drop ΔV_{AC} on a defined length of the conductor under test. Under sinusoidal AC supply, it is also needed to measure the phase shift φ between the voltage drop and the current, so that the AC resistance can be determined as $R_{AC} = (\Delta V_{AC}/I_{AC})\cdot\cos\varphi$.

4. Experimental Setup

According to the developments presented in Section 3, in order to calculate the AC resistance R_{AC} of the conductor, the core must be characterized. Therefore, the fields *B* and *H* as well the loss angle δ_{eff} and the complex magnetic permeability of the core $\overline{\mu}_{rs}$ must be characterized. This section describes the experimental setup used for this purpose.

This work analyses two ACSR conductors, whose main parameters are summarized in Table I.

Table I. Parameters of the Studied two-layer ACSR conductors

NAME	135 AL1 (two-layer)	CROCUS 288 (two-layer)
Lay length of the first layer, λ [cm]	15	22
Lay length of the second layer, λ [cm]	21.8	25.5
Core cross-section area, A_s [mm^2]	22	54.55
R_{DC} (20ºC) [Ω/km]	0.20565	0.11694
Number of core strands	7	7
Number of Al strands	10+16=26	12+18=30
Al strands diameter [mm]	2.57	3.15
Two-layer outer diameter, D2 [mm]	16.3	22
Single-layer outer diameter, D1 [mm]	11.3	15.75
Steel strands diameter [mm]	2.0	3.15
Mass [kg/m]	0.1728 (Core)	1.073 (Total)

Fig. 2 shows a sketch of the experimental setup used to characterize the core material. To this end, a sample of the conductor of approximately 1.195 m was considered, and the Al layers were removed to characterize the core.

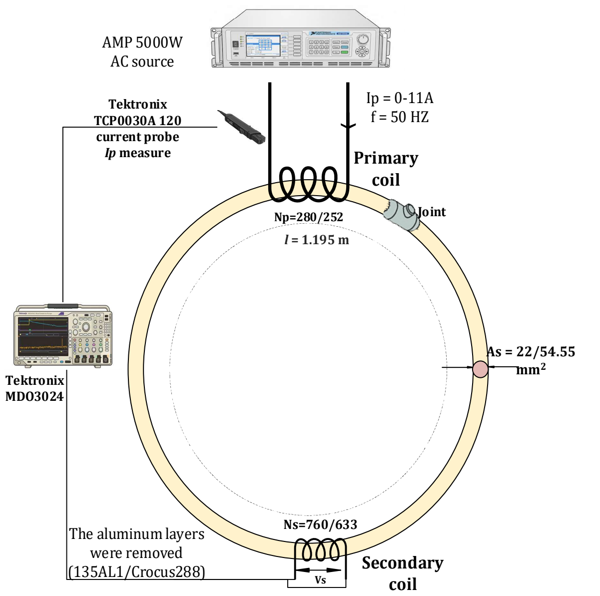

Fig. 2. Experimental setup used to determine the B and H fields as well as δ_{eff}, $\mu_{r,eff}'$ and $\mu_{r,eff}''$. This setup was used to characterize the core of the Crocus 288 and 135Al1conductors.

The sensitivity of the voltage reading at the secondary coil is affected by the background noise, mainly at low primary current (low H_p values). After several trials, the number of turns in the primary coil was settled to N_p = 280/252 for 135AL1/Crocus, while the number of turns in the secondary coil was settled to N_s = 760/633 for 135AL1/Crocus. The core was kept at a constant temperature of 59ºC during the experiments by means of a Digiheat 1000 W muffle (1000 W, ambient temperature + 5ºC to 150ºC, JP Selecta, Barcelona, Spain).

Fig. 3 shows the experimental setup described in Fig. 2 when placed inside the muffle.

Fig. 3. Photograph of the experimental setup for determining the δ_{eff}, $\mu_{r,eff}'$ and $\mu_{r,eff}''$ for cores of the conductors Crocus 288 and 135AL1 conductors.

An APM SP300VAC-5000W (5000 W, 0-300 V, 0-1000 Hz, AMP, Louisville, Colorado, USA) programmable AC source was used to supply the circuit shown in Fig. 1. A TCP0030A AC/DC current probe (30 A-RMS, bandwidth > 120 MHz, accuracy better than 1% DC gain error, Tektronix, Beaverton, Oregon, USA) was used to measure the current in the primary coil. The secondary voltage was acquired with a MD03024 oscilloscope (4 channels, 200 MHz, 2.5 GSamples/s, up to 11 bits, Tektronix, Beaverton, Oregon, USA).

Fig. 4 and Fig. 5 the layout and photographs of the analyzed conductors, i.e., the 135AL1 with 7 strands in the core and two layers of 10 and 16 aluminium strands, and the Crocus288 with 7 strands in the core and two layers of 12 and 18 aluminium strands.

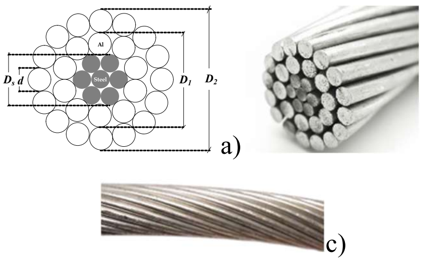

Fig. 4. ACSR 135AL1 conductor. a) Cross-section sketch. b) Cross-section photograph. c) Conductor photograph.

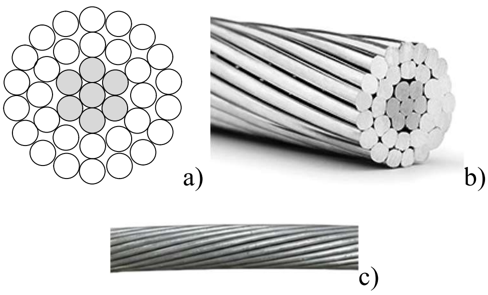

Fig. 5. Crocus 288 conductor. a) Cross-section sketch. b) Cross-section photograph. c) Conductor photograph.

To determine the AC resistance of the conductors, they were tested in a loop when supplied using a high-current transformer by applying different current levels, as shown in Fig. 6. Note that the full conductors were tested, including the core and the two layers of aluminum strands.

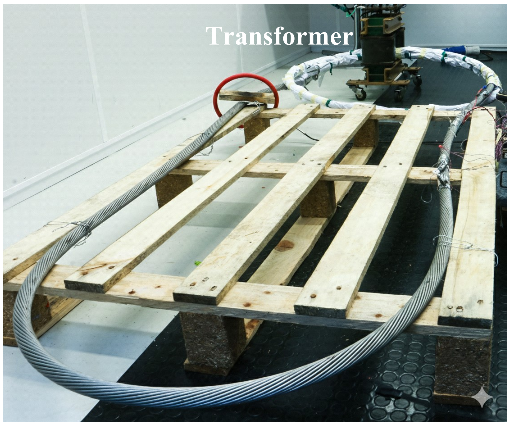

Fig. 6. Experimental setup for the conductor loop test, measuring AC resistance as a function of temperature across varying current levels.

5. Results and Discussion

This section describes the experimental results and the results obtained from Methods #1 and #2 and compare them against those of the 4-wire method.

The first step was to determine experimentally the parameters H_p, tan(δ_{eff}) and $\mu_{r,eff}'$ of the steel cores. These results are shown in Figs. 7 and 8 for the 135AL1 and

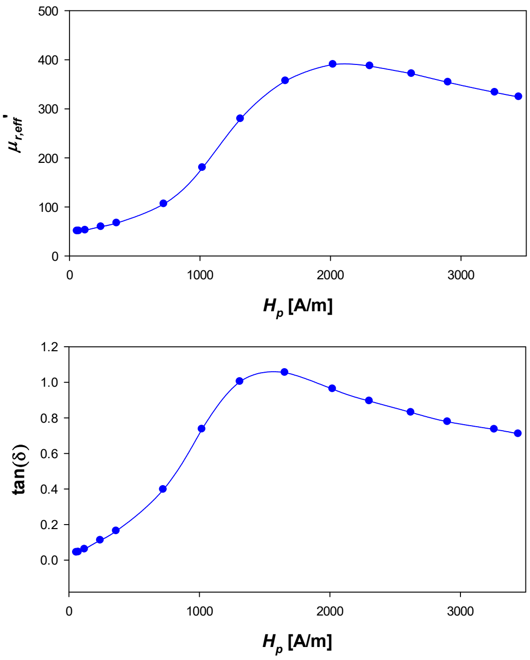

Fig. 7. ACSR 135AL1 conductor (double layer). Experimental values of tan(δ_{eff}) and $\mu_{r,eff}'$ versus H_p at 59ºC.

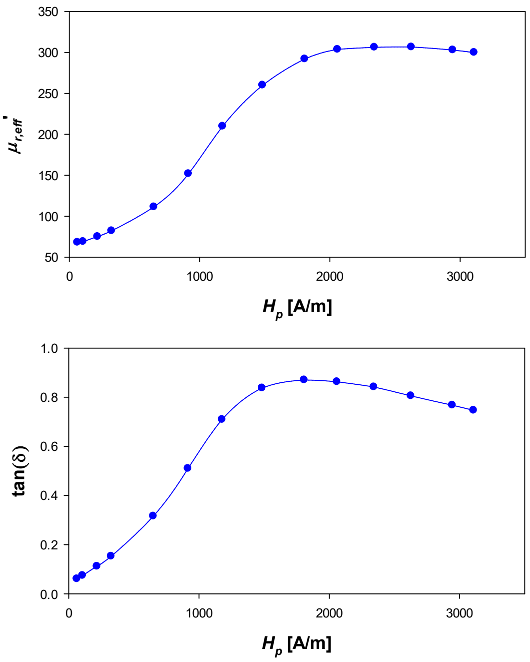

Fig. 8. Crocus288 conductor (double layer). Experimental values of tan(δ_{eff}) and $\mu_{r,eff}'$ versus H_p at 59ºC.

Once the dependencies $\delta_{\mathrm{eff}}(H_p)$ and $\mu_{\mathrm{r,eff}}'(H_p)$ are known, Methods #1 and #2 can be applied.

Table II summarizes the results attained with the 135AL1 and Crocus288 ACSR conductors at different current levels.

Table II. Parameters of the Studied two-layer ACSR conductors

ACSR 135AL1 two-layer ACSR conductor			
Current (A)	R_{AC} (μΩ/m)		
	Method #1	Method#2	Reference 4-wire
50A	237.8	239.7	250.7
100A	237.8	239.7	250.5
150A	237.8	239.7	246.6
200A	237.8	239.7	244.3
250A	237.8	239.7	243.2
300A	237.8	239.7	242.5
350A	237.8	239.7	241.8
400A	237.8	239.7	242.0
R_{DC} at 59ºC	237.8		
Crocus288 two-layer ACSR conductor			
Current (A)	R_{AC} (μΩ)		
	Method #1	Method#2	Reference 4-wire
200A	136.2	137.4	143.4
250A	136.2	137.4	142.9
300A	136.2	137.5	141.8
350A	136.3	137.5	140.1
400A	136.3	137.5	140.0
450A	136.3	137.6	138.9
500A	136.3	137.9	138.6
550A	136.3	138.2	137.9
600A	136.3	138.3	138.3
R_{DC} at 59ºC	136.2		

For both conductors, different current ranges were chosen due to their differing ampacities. While both have a maximum allowable operating temperature of approximately 90°C, the Crocus288 conductor has a significantly higher ampacity and exhibits minimal temperature rise at lower currents. To capture meaningful heating profiles up to the 90°C limit, the test range for Crocus288 was set from 200 A to 600 A, whereas the ACSR 135AL1 was tested from 50 A to 400 A. A step increment of 50 A was maintained for both tests.

The results presented in Table II show discrepancies between Methods #1 and #2 and the 4-wire method, especially at low current levels. While according to Methods #1 and #2 the AC resistance is almost independent on the current level, according to the 4-wire method the AC resistance decreases as the current increases. This can be due to the fact that layers 1 and 2 do not carry the same amount of current, so there is only a partial magnetic flux cancellation.

Fig. 9 shows the results of the loop tests performed on the conductors at different current levels. This figure clearly shows that the AC resistance (measured with the 4-wire method) of the two-layer conductors increases with the temperature but it also depends on the level of the current. This also reflects the non-linear dependency of AC resistance on current. At lower currents, the resistance is highly sensitive to current changes. However, at higher levels, this dependency weakens, causing the resistance to stabilize across the final test intervals.

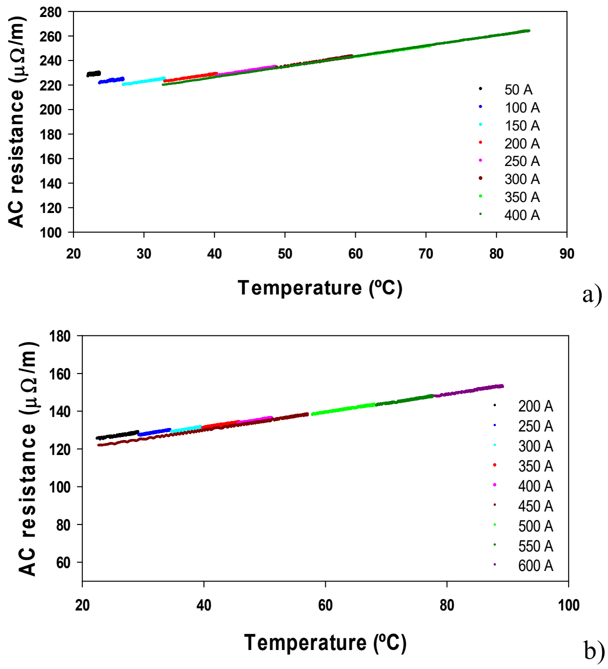

Fig. 9. Temperature and current dependency of the AC resistance. a) ACSR 135AL1 two-layer ACSR conductor. b) Crocus288 two-layer ACSR conductor.

6. Conclusion

Aluminum conductors steel-reinforced (ACSR), have been widely used for more than one century in overhead power lines. They are probably the most applied conductors in transmission lines. Due to the steel core magnetization, they present a non-linear behavior. This is reflected in a current dependency of the AC resistance.

This paper has analyzed the particular case of two-layer ACSR conductors, showing that even in this case, the magnetic flux generated by the two aluminum layers, that are stranded in opposite directions, is not completely cancelled. This effect is attributed to the fact that the currents in the two layers are not equal and thus, the magnetic flux is not cancelled. This effect is more evident when the conductors are lightly loaded.

The experimental results presented here reveal that even in two-layer conductors, the AC resistance depends on the current level, this effect being notorious at low current levels and decreasing as high current levels. It is also shown that the methods for modelling the AC resistance of steel-core conductors found in the literature do not provide an accurate representation of this phenomenon for low current levels, while the 4-wire Kelvin method is more accurate but difficult to apply in operating power lines.

Acknowledgement

This project received funding from grant PID2023-147016OB-I00, by MICIU/AEI/10.13039/501100011033/ and by ERDF "A way of making Europe," by the European Union and from the Agència de Gestió d'Ajuts Universitaris i de Recerca-AGAUR (2021 SGR 00392, 2024 DI 010).

References

[1] J.-R. Riba, Y. Liu, M. Moreno-Eguilaz, and J. Sanllehí, "On-Line Core Losses Determination in ACSR Conductors for DLR Applications," *Mater. 2022, Vol. 15, Page 6143*, vol. 15, no. 17, p. 6143, Sep. 2022.

[2] R. A. Meyberg, F. M. Absi Salas, L. A. M. C. Domingues, M. A. Sens, M. T. Correia de Barros, and A. C. S. Lima, "Magnetic properties of an ACSR conductor steel core at temperatures up to 230 ∘C and their impact on the transformer effect," *IET Sci. Meas. Technol.*, vol. 15, no. 2, pp. 143–153, Mar. 2021.

[3] J.-R. Riba, "The Role of AC Resistance of Bare Stranded Conductors for Developing Dynamic Line Rating Approaches," *Appl. Sci.*, vol. 14, no. 19, p. 8982, Oct. 2024.

[4] V. T. Morgan, "Electrical characteristics of steel-cored aluminium conductors," *Proc. Inst. Electr. Eng.*, vol. 112, no. 2, p. 325, 1965.

[5] Morgan VT and Price CF, "Magnetic properties in axial 50 Hz fields of steel core wire for overhead-line conductors," *Proc. Inst. Electr. Eng.*, vol. 116, no. 10, pp. 1681–1694, 1969.

[6] B. S. Howington, "AC Resistance of ACSR—Magnetic and Temperature Effects: Prepared by a Task Force of the Working Group on Calculation of Bare Overhead Conductor Temperatures," *IEEE Power Eng. Rev.*, vol. PER-5, no. 6, pp. 67–68, 1985.

[7] IEEE Std 738-2012, "IEEE Standard for Calculating the Current-Temperature of Bare Overhead Conductors," New York, USA, 2012.

[8] J. S. Barrett, O. Nigol, C. J. Fehervari, and R. D. Findlay, "A new model of AC resistance in acsr conductors," 1986.

[9] V. T. Morgan, "The Current Distribution, Resistance and Internal Inductance of Linear Power System Conductors—A Review of Explicit Equations," *IEEE Trans. Power Deliv.*, vol. 28, no. 3, pp. 1252–1262, Jul. 2013.

[10] V. T. Morgan, B. Zhang, and R. D. Findlay, "Effects of temperature and tensile stress on the magnetic properties of a steel core from an ACSR conductor," *IEEE Trans. Power Deliv.*, vol. 11, no. 4, pp. 1907–1913, 1996.

[11] X. Li, J. Guo, J. Bi, and H. Li, "Development of 3 kV low-frequency induction voltage divider using two-stage excitation," *High Volt.*, vol. 10, no. 4, pp. 998–1009, Aug. 2025.

[12] D. J. Griffiths, *Introduction to Electrodynamics*. New Jersey, USA: Prentice Hall, 1999.

[13] Cigré 345, "Alternating current (AC) resistance of helically stranded conductors." Cigré, Paris, pp. 1–59, 2008.

[14] Cigre, "Basic principles and practical methods to measure the AC and DC resistance of conductors of power cables - TB 894," 2023.